Monthly Notices
of the
ROYAL ASTRONOMICAL SOCIETY

MNRAS **462,** 3912–3917 (2016)
Advance Access publication 2016 August 1

doi:10.1093/mnras/stw1900

Experimental radiative lifetimes for highly excited states and calculated oscillator strengths for lines of astrophysical interest in singly ionized cobalt (Co II)

P. Quinet,[1,2]★ V. Fivet,[1] P. Palmeri,[1] L. Engström,[3] H. Hartman,[4,5] H. Lundberg[3] and H. Nilsson[4]

[1]*Physique Atomique et Astrophysique, Université de Mons, B-7000 Mons, Belgium*
[2]*IPNAS, Université de Liège, Sart Tilman, B-4000 Liège, Belgium*
[3]*Department of Physics, Lund University, Box 118, SE-221 00 Lund, Sweden*
[4]*Lund Observatory, Lund University, Box 43, SE-221 00 Lund, Sweden*
[5]*Material Sciences and Applied Mathematics, Malmö University, SE-205 06 Malmö, Sweden*

Accepted 2016 July 28. Received 2016 July 28; in original form 2016 May 17

ABSTRACT

This work reports new experimental radiative lifetimes and calculated oscillator strengths for transitions of astrophysical interest in singly ionized cobalt. More precisely, 19 radiative lifetimes in Co^+ have been measured with the time-resolved laser-induced fluorescence technique using one- and two-step excitations. Out of these, seven belonging to the high lying $3d^7(^4F)4d$ configuration in the energy range 90 697–93 738 cm^{-1} are new, and the other 12 from the $3d^7(^4F)4p$ configuration with energies between 45 972 and 49 328 cm^{-1} are compared with previous measurements. In addition, a relativistic Hartree–Fock model including core-polarization effects has been employed to compute transition rates. Supported by the good agreement between theory and experiment for the lifetimes, new reliable transition probabilities and oscillator strengths have been deduced for 5080 Co II transitions in the spectral range 114–8744 nm.

Key words: atomic data – atomic processes.

1 INTRODUCTION

The final stage of exothermal elemental production in stars is the iron-group elements. The even-*Z* atoms are produced by consecutive capture of helium nuclei, and named α-elements. The production of the odd-*Z* elements is not as well constrained, and does not follow the abundance trends of the α-elements, indicating non-common production sites. As a result of this nucleosynthesis in the interior of stars, the even-*Z* nuclei such as Ca, Ti, Cr and Fe have a higher cosmic abundance compared to the odd-*Z* nuclei located in between. However, the astrophysical interest for the odd-*Z* iron-group elements has increased in recent years. In the present project, we target atomic data for Co II ($Z = 27$). Cobalt is believed to be produced primarily in Type II supernova, and also to a lesser extent in Type Ia supernova (Woosley & Weaver 1995; Bravo & Martinez-Pinedo 2012; Battistini & Bensby 2015). Abundance determinations in stars serve as important tests of the stellar evolution and supernova explosion models (Pagel 2009). Furthermore, high-excitation spectral lines have additional diagnostic value, since they can be used to benchmark non-local thermodynamical equilibrium (non-LTE) modelling of stellar atmospheres. Along with the development of 3D model atmospheres, a trustworthy non-LTE treatment is the current challenge for accurate stellar abundances. High-precision atomic data for selected lines are important for this development (Lind, Bergemann & Asplund 2012).

In the case of cobalt, a big effort was recently made by Lawler, Sneden & Cowan (2015) to provide improved oscillator strengths for about 900 lines belonging to the first spectrum (Co I). These were deduced from emission branching fractions measured from hollow cathode lamp spectra recorded using a Fourier transform spectrometer and a high-resolution echelle spectrograph combined with radiative lifetimes determined by the time-resolved laser-induced fluorescence (TR-LIF) technique.

Concerning the second spectrum (Co II), several papers have reported experimental determinations of radiative data. Lifetime measurements have been performed by Pinnington, Lutz & Carriveau (1974) and Sørensen (1979) using the beam-foil technique and by Salih, Lawler & Whaling (1985) and Mullman et al. (1998a) using TR-LIF. Experimental transition probabilities were reported for 41 spectral lines by Salih et al. (1985), Crespo López-Urrutia et al. (1994) and Mullman et al. (1998b) by combining branching fraction

★ E-mail: pascal.quinet@umons.ac.be

measurements with available lifetimes. Theoretical data have been published by Raassen, Pickering & Uylings (1998) who computed oscillator strengths for a large number of Co II lines using the method of orthogonal operators. However, all these studies were limited to radiative decays from the odd-parity $3d^7 4p$ configuration to lower states belonging to the $3d^8$ and $3d^7 4s$ even-parity configurations. More extensive calculations are reported by Kurucz (2011).

The main goal of the present work is to extend the knowledge of radiative data to higher energy states and to provide a consistent set of transition rates for a large number of spectral lines in singly ionized cobalt. More precisely, new experimental lifetime measurements were performed by TR-LIF for 12 energy levels belonging to the $3d^7 4p$ odd-parity configuration and seven energy levels belonging to the $3d^7 4d$ even-parity configuration using one- and two-step excitations, respectively. In addition, transition probabilities and oscillator strengths were computed for 5080 Co II lines in a wide spectral region, from ultraviolet to infrared, using a pseudo-relativistic Hartree–Fock model including core-polarization effects.

2 RADIATIVE LIFETIME MEASUREMENTS

The experimental set-up for one- and two-step experiments at the Lund High Power Laser Facility has recently been described in detail (Engström et al. 2014; Lundberg et al. 2016). For an overview we refer to fig. 1 in Lundberg et al. (2016), and here we mainly give the most important details. The Co^+ ions were produced by focusing 10 ns long pulses from a frequency doubled Nd:YAG laser on to a rotating Co target placed in a vacuum chamber where the pressure was about 10^{-4} mbar. The Co plasma created in the ablation process was crossed by one or two laser beams 5 mm above the target.

Both laser systems consisted of a frequency doubled Nd:YAG laser (Continuum NY-82) pumping a Continuum Nd-60 dye laser, mostly operating with DCM dye. For the wavelengths above 225 nm the second (or only) laser used oxazin dye instead. In all measurements the final output from the dye lasers was frequency tripled using KDP and BBO crystals. The pulse length from the first laser was 10 ns, whereas for the second (or only) laser we achieved a pulse length after tripling of about 1 ns by injection seeding and compressing the output from the Nd:YAG laser. The compressor utilized stimulated Brillouin scattering in water.

The fluorescence emitted by the Co^+ ions was dispersed by a 1/8 m grating monochromator, with its 0.1 mm wide entrance slit oriented parallel to the excitation laser beam, registered by a fast microchannel-plate photomultiplier tube (Hamamatsu R3809U) and finally digitized by a Tektronix DPO 7254 oscilloscope. The oscilloscope, with 2.5 GHz analogue band width, sampled the decay in 50 ps intervals. All measurements used the second spectral order, giving an observed line width of about 0.5 nm. The excitation laser pulse shape was recorded simultaneously using a fast photodiode and digitized in a second channel on the oscilloscope. The final decay curves and pulse shape were obtained by averaging over 1000 laser pulses. The code DECFIT (Palmeri et al. 2008) was then used to extract the lifetimes by fitting a single exponential function convoluted by the measured shape of the second-step laser pulse and a background function to the observed decay.

Table 1 gives the wavelengths for the excitation and detection channels used in the single-step measurements. All two-step excitations started from the $3d^7 4p\ z^5G_5$ level at 47 346 cm^{-1}, and the excitation and detection channels used are listed in Table 2.

For the two-step measurements several special experimental aspects have to be considered. Before every measurement the delay between the two lasers was adjusted so that the short pulse from

Table 1. Single-step measurements for $3d^7(^4F)4p$ levels in Co II.

Level	Energy[a] E (cm^{-1})	Starting level[a] E (cm^{-1})	Excitation[b] λ_{air} (nm)	Detection[c] λ_{air} (nm)
$z\ ^5F^\circ_3$	45 972.036	0.000	217.45	238, 241
$z\ ^5D^\circ_4$	46 320.832	0.000	215.82	232, 236
$z\ ^5F^\circ_2$	46 452.700	1597.197	222.86	239
$z\ ^5D^\circ_3$	47 039.105	0.000	212.52	232, 235
$z\ ^5G^\circ_6$	47 078.494	3350.494	228.62	229[d]
$z\ ^5G^\circ_5$	47 345.845	0.000	211.15	231
$z\ ^5D^\circ_2$	47 537.365	950.324	214.58	233, 235
$z\ ^5G^\circ_4$	47 807.493	950.324	213.35	228, 231, 269
$z\ ^5G^\circ_3$	48 150.940	950.324	211.79	231
$z\ ^5G^\circ_2$	48 388.442	1597.197	213.65	231
$z\ ^3G^\circ_4$	49 348.304	950.324	206.55	253

[a]NIST compilation (Kramida et al. 2014).
[b]All levels were excited using the third harmonic of the dye laser.
[c]All fluorescence measurements were performed in the second spectral order.
[d]Corrected for scattered laser light at the same wavelength.

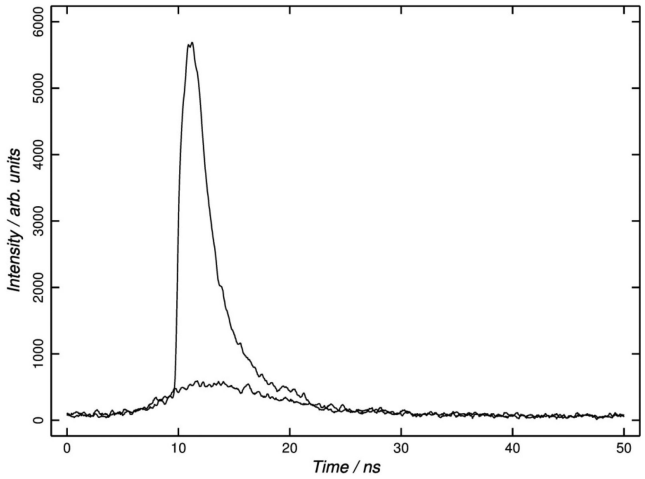

Figure 1. Decay of the $4d^7(^4F)4d\ e^5H_6$ level at 236 nm perturbed by the fluorescence from the $4d^7(^4F)4p\ z^5G_5$ level at 231 nm excited by the first-step laser. The lower curve shows a measurement at 236 nm with the second-step laser turned off, revealing the contribution from z^5G_5.

second laser coincided with the maximum population of the intermediate $3d^7 4p\ z^5G_5$ level. The latter was found by observing the maximum in the fluorescence light from this level at either 231 or 266 nm. When detecting the decay of the final $3d^7 4d$ levels two types of line blending can occur. The very intense light emitted by the intermediate level at 231 nm results in a time-dependent background observable in a several nm wide wavelength region. The lifetime of z^5G_5 is about 3 ns but the fluorescence signal extends over more than 10 ns due to the width of the first-step laser pulse. This blending problem can, however, be accurately handled by recording the background signal with the second-step laser turned off and then subtracting this from the observed final decay. This technique is illustrated in Fig. 1, and the measurements influenced by this effect are marked in Table 2. A more difficult problem is that the level under investigation usually decays along several cascade chains where one or more secondary (4s-4p) channels may occur close to the measured decay. Contrary to blending from the intermediate level the cascades are of much lower intensity, and hence the blending has to be almost perfect in wavelength to cause a serious problem. Since

Table 2. Two-step measurements for $3d^7(^4F)4d$ levels in Co II.

Level	Energy[a] E (cm^{-1})	Excitation[b] λ_{air} (nm)	Detection[c] λ_{air} (nm)
e $^5G_5$	90 697.464	230.60	220
e $^5H_6$	90 975.540	229.13	236[d]
e $^5G_4$	91 049.431	228.74	221, 223
e $^3G_5$	91 326.932	227.37	222
e $^3H_6$	91 623.455	225.78	232[d]
e $^5H_5$	91 646.447	225.66	228[d]
f $^3F_4$	93 738.788	215.48	237[d]

[a]NIST compilation (Kramida et al. 2014).
[b]All levels were excited from the intermediate 4p z $^5G_5$ level at 47 346 cm^{-1}, given in Table 1, using the third harmonic of the dye laser.
[c]All fluorescence measurements were performed in the second spectral order.
[d]Corrected for the strong fluorescence background from the intermediate level at 231 nm, as discussed in the text and illustrated in Fig. 1.

Table 3. Experimental and calculated radiative lifetimes (in ns) for selected energy levels belonging to the $3d^74p$ and $3d^74d$ configurations of Co II.

Level	Energy[a] (cm^{-1})	Experiment		Calculations	
		Previous	This work	This work	Kurucz[d]
4p z $^5F_5$	45 197.711	3.5 ± 0.2[b]		2.97	2.79
4p z $^5F_4$	45 378.754	3.5 ± 0.2[b]		3.07	2.87
4p z $^5F_3$	45 972.036	3.7 ± 0.2[b]	3.21 ± 0.15	3.03	2.85
4p z $^5D_4$	46 320.832	3.3 ± 0.2[b]	3.10 ± 0.15	3.02	2.82
4p z $^5F_2$	46 452.700	3.0 ± 0.2[b]	3.12 ± 0.15	3.00	2.83
4p z $^5F_1$	46 786.409	3.4 ± 0.2[b]		2.99	2.83
4p z $^5D_3$	47 039.105	3.4 ± 0.2[b]	3.11 ± 0.15	3.03	2.82
4p z $^5G_6$	47 078.494	3.0 ± 0.3[b]	2.70 ± 0.15	2.54	2.48
4p z $^5G_5$	47 345.845	3.2 ± 0.2[b]	2.93 ± 0.15	2.72	2.65
4p z $^5D_2$	47 537.365	3.3 ± 0.2[b]	3.04 ± 0.20	3.03	2.83
4p z $^5G_4$	47 807.493	3.0 ± 0.2[b]	2.84 ± 0.15	2.67	2.60
4p z $^5D_1$	47 848.781	3.4 ± 0.2[b]		3.05	2.84
4p z $^5G_3$	48 150.940	3.1 ± 0.2[b]	2.86 ± 0.15	2.65	2.58
4p z $^5G_2$	48 388.442	3.2 ± 0.2[b]	2.84 ± 0.15	2.63	2.57
4p z $^5G_5$	48 556.052	3.6 ± 0.2[c]	2.84 ± 0.15	2.63	3.07
4p z $^3G_4$	49 348.304	3.3 ± 0.2[c]	3.03 ± 0.15	2.78	2.58
4p z $^3F_4$	49 697.683	2.9 ± 0.2[c]		2.54	2.46
4p z $^3G_3$	50 036.348	3.5 ± 0.2[c]		3.01	2.79
4p z $^3F_3$	50 381.724	2.9 ± 0.2[c]		2.44	2.35
4p z $^3F_2$	50 914.325	2.9 ± 0.2[c]		2.28	2.13
4p z $^3D_3$	51 512.268	2.3 ± 0.2[c]		1.94	1.83
4p z $^3D_2$	52 229.725	2.3 ± 0.2[c]		1.97	1.86
4p z $^3D_1$	52 684.634	2.4 ± 0.2[c]		1.98	1.87
4d e $^5G_5$	90 697.464		1.41 ± 0.10	1.44	1.37
4d e $^5H_6$	90 975.540		1.57 ± 0.10	1.42	1.36
4d e $^5G_4$	91 049.431		1.35 ± 0.10	1.38	1.35
4d e $^3G_5$	91 326.932		1.44 ± 0.10	1.43	1.41
4d e $^3H_6$	91 623.455		1.36 ± 0.10	1.44	1.39
4d e $^5H_5$	91 646.447		1.52 ± 0.10	1.40	1.35
4d f $^3F_4$	93 738.788		1.58 ± 0.10	1.56	1.64

[a]NIST compilation (Kramida et al. 2014).
[b]Salih et al. (1985).
[c]Mullman et al. (1998a,b).
[d]Kurucz (2011).

such blends cannot be compensated for, we carefully investigated this possibility before choosing the appropriate channels to use, as discussed in Lundberg et al. (2016).

The final lifetimes are given in Table 3 and represent the averages of 10–20 measurements performed over several days. The quoted uncertainties are mainly based on the variation between the different measurements (Palmeri et al. 2008).

Table 4. Radial parameters adopted in the HFR+CPOL calculations for the $3d^8$, $3d^74s$, $3d^75s$ and $4d^74d$ even-parity configurations of Co II.

Config.	Parameter	Ab initio (cm^{-1})	Fitted (cm^{-1})	Ratio	Note[a]
$3d^8$	E_{av}	20 895	11 615		
	$F^2(3d,3d)$	84 335	70 521	0.836	
	$F^4(3d,3d)$	52 008	43 842	0.843	
	α	0	69		
	β	0	294		
	ζ_{3d}	474	470	0.992	
$3d^74s$	E_{av}	26 351	27 378		
	$F^2(3d,3d)$	92 176	79 060	0.858	
	$F^4(3d,3d)$	57 195	51 853	0.907	
	α	0	92		
	β	0	−1115		
	ζ_{3d}	526	508	0.967	
	$G^2(3d,4s)$	10 203	7908	0.775	
$3d^75s$	E_{av}	103 359	105 208		
	$F^2(3d,3d)$	93 461	78 524	0.840	
	$F^4(3d,3d)$	58 056	52 676	0.907	
	α	0	74		
	β	0	−1053		
	ζ_{3d}	531	479	0.902	
	$G^2(3d,5s)$	1846	1654	0.896	
$3d^74d$	E_{av}	108 802	111 591		
	$F^2(3d,3d)$	93 577	77 104	0.824	
	$F^4(3d,3d)$	58 134	48 229	0.830	
	α	0	93		
	β	0	−5		
	ζ_{3d}	532	556	1.046	
	ζ_{4d}	13	13	1.000	F
	$F^2(3d,4d)$	4680	3850	0.823	R1
	$F^4(3d,4d)$	1705	1403	0.823	R1
	$G^0(3d,4d)$	1924	1103	0.573	R2
	$G^2(3d,4d)$	1635	938	0.573	R2
	$G^4(3d,4d)$	1139	654	0.573	R2

[a]F: fixed parameter value; R*n*: fixed ratio between these parameters.

3 OSCILLATOR STRENGTH CALCULATIONS

To model the atomic structure and to compute the radiative decay rates in singly ionized cobalt, we considered a relativistic Hartree–Fock (HFR) model using the suite of computer codes originally developed by Cowan (1981), and subsequently modified to take core-polarization into account, giving rise to the HFR+CPOL approach (see e.g. Quinet et al. 1999, 2002). In the present case, the configurations explicitly included in the configuration interaction expansions were the following: $3d^8 + 3d^74s + 3d^75s + 3d^74d + 3d^75d + 3d^64s^2 + 3d^64s5s + 3d^64s4d + 3d^64s5d + 3d^54s^24d + 3d^54s^25s$ (even parity) and $3d^74p + 3d^75p + 3d^74f + 3d^75f + 3d^64s4p + 3d^64s5p + 3d^64s4f + 3d^64s5f + 3d^54s^24p + 3d^54s^24f$ (odd parity). The ionic core considered for the core-polarization model potential and the correction to the dipole operator was a vanadium-like core, i.e. a $3d^5$ Co^{4+} core. The dipole polarizability for such a core is 1.01 a_0^3 according to Fraga, Karwowski & Saxena (1976). For the cut-off radius, we used the HFR mean value of the outermost 3d core orbital, i.e. 1.00 a_0.

Some radial integrals, considered as free parameters, were then adjusted with a least-squares optimization program minimizing the discrepancies between the calculated Hamiltonian eigenvalues and the experimental energy levels from the NIST data base (Kramida et al. 2014). In this compilation, Co II energy levels from Pickering

Table 5. Radial parameters adopted in the HFR+CPOL calculations for the $3d^74p$ and $3d^64s4p$ odd-parity configurations of Co II.

Config.	Parameter	Ab initio (cm^{-1})	Fitted (cm^{-1})	Ratio	Note[a]
$3d^74p$	E_{av}	66 556	68 604		
	F^2(3d,3d)	92 841	78 444	0.845	
	F^4(3d,3d)	57 642	52 043	0.903	
	α	0	89		
	β	0	−1001		
	ζ_{3d}	529	519	0.981	
	ζ_{4p}	364	438	1.203	
	F^2(3d,4p)	14 303	12 883	0.901	
	G^1(3d,4p)	5670	4830	0.852	
	G^3(3d,4p)	4579	3205	0.700	
$3d^64s4p$	E_{av}	109 002	117 652		
	F^2(3d,3d)	100 034	80 027	0.800	F
	F^4(3d,3d)	62 434	49 947	0.800	F
	α	0	0		F
	β	0	0		F
	ζ_{3d}	583	583	1.000	F
	ζ_{4p}	487	487	1.000	F
	F^2(3d,4p)	16 205	14 190	0.876	R
	G^2(3d,4s)	10 171	8906	0.876	R
	G^1(3d,4p)	5922	5186	0.876	R
	G^3(3d,4p)	5025	4400	0.876	R
	G^1(4s,4p)	45 716	40 030	0.876	R

[a]F: fixed parameter value; R: fixed ratio between these parameters.

et al. (1998) and from Pickering (1998) were increased by 6.7 parts in 10^8 to account for the calibration correction found by Nave & Sansonetti (2011). Moreover, the additive constant '+x' introduced by Pickering et al. (1998) for the $3d^7(^2F)4s$ and $3d^7(^2F)4p$ energy levels was eliminated by adjusting these levels to fit the wavelengths of 20 observed intersystem spectral lines. Four of these lines were measured by Pickering et al. (1998) while the other 16 lines were observed by Iglesias (1979). For the $3d^8$, $3d^74s$, $3d^75s$ and $3d^74d$ even-parity configurations, the average energies (E_{av}), the electrostatic direct (F^k) and exchange (G^k) integrals, the spin-orbit (ζ_{nl}) and the effective interaction (α, β) parameters were allowed to vary during the fitting process. In addition, the average energies for the $3d^75d$ and $3d^64s^2$ configurations were also included in the adjustment. For the few experimental even levels located above 111 000 cm^{-1} it was very difficult to establish an unambiguous correspondence with the calculated values so these levels were omitted in the semi-empirical process. In the odd parity configurations, only experimental levels located below 90 000 cm^{-1} were used to optimize some radial parameters in the $3d^74p$ and $3d^64s4p$ configurations. The fitting process was not applied to the highly excited levels reported in the NIST compilation as belonging to $3d^75p$ and $3d^74f$ configurations because most of them appeared to be very strongly mixed with experimentally unknown levels. For both parities, all the other radial electrostatic interaction parameters were fixed at 80 per cent of their ab initio HFR values.

The numerical values of the parameters adopted in the present calculations are reported in Tables 4 and 5 for even-parity and odd-parity configurations, respectively. This semi-empirical process led to average deviations with experimental energy levels equal to 110 cm^{-1} (158 levels, 30 fitted parameters) for the even parity, and 127 cm^{-1} (114 levels, 12 fitted parameters) for the odd parity.

4 RESULTS AND DISCUSSION

The computed radiative lifetimes obtained in the present work are compared with the available experimental values in Table 3. Our experimental values agree within the mutual error bars with Salih et al. (1985) and Mullman et al. (1998a). However, there is a tendency for our new values to be somewhat shorter. This could probably be explained by our shorter pulse length and better time resolution in the detection system. As shown in this table, the overall agreement between theory and experiment is good, the average relative differences being found to be equal to 12, 17 and 5 per cent, when considering the lifetime measurements due to Salih et al. (1985), Mullman et al. (1998a) and the present study, respectively. For comparison, Table 3 includes the theoretical lifetimes obtained by Kurucz (2011). This work also used a semi-empirical approach based on a superposition of configurations calculation with a modified version of the Cowan (1981) codes and experimental level energies. We note a very good qualitative agreement between the two calculations, but that our new results, with two exceptions, are consistently 5 per cent longer and closer to the experimental values.

Table 6 gives the HFR+CPOL oscillator strengths (log *gf*) and weighted transition probabilities (*gA*), together with the experimental energies of the lower and upper levels and the corresponding wavelengths for 5080 Co II spectral lines from 114 to 8744 nm. These correspond to all the electric dipole transitions involving the experimentally known levels (Pickering 1998; Pickering et al. 1998; Kramida et al. 2014) for which log *gf* is larger than −4. In the last column of the table, we also give the value of the cancellation factor (CF), as defined by Cowan (1981). Very small values of this factor (typically <0.05) indicate strong cancellation effects in the calculation of the line strengths and the corresponding transition rates can be affected by larger uncertainties and should be considered with some care. This concerns about 25 per cent of the lines listed in Table 6, the large majority of them being characterized by weak oscillator strengths (log $gf < -2$).

When comparing the results obtained with our computational approach with the previously published decay rates, we find an overall good agreement. This is illustrated in Figs 2–5, where our calculations are compared with the experimental data reported by Salih et al. (1985), Crespo López-Urrutia et al. (1994), Mullman et al. (1998a,b) and those obtained theoretically by Raassen et al. (1998). More precisely, as shown in Fig. 2, we obtain a mean ratio of 1.036 ± 0.205 when comparing our transition probabilities with those of Salih et al. (1985), who combined lifetime values obtained by TR-LIF with branching fractions measured on spectra recorded with the 1-m Fourier-transform spectrometer at the Kitt Peak National Observatory, to deduce the decay rates for 41 transitions depopulating the $3d^74p$ z^5F, z^5D and z^5G levels. Fig. 3 shows a slightly larger scatter between our calculations and the transition probabilities published by Crespo López-Urrutia et al. (1994). Here the mean ratio $gA_{\rm Thiswork}/gA_{\rm Crespo}$ is equal to 1.098 ± 0.493. However, it is worth noting that the *gA*-values obtained by the latter authors were deduced from the combination of branching ratio measurements with available experimental lifetimes for the $3d^74p$ z^5F, z^5D, z^5G levels (Pinnington, Lutz & Carriveau 1973; Pinnington et al. 1974; Salih et al. 1985) but also with estimated lifetimes for the z^3G, z^3F and z^3D levels from the measurement of total intensity of all lines of each of these levels under the assumption of almost equal population. The branching fractions were found using intensity measurements with a special hollow electrode radio frequency discharge and using a phase method with a modified wall-stabilized arc in a spectrointerferometric arrangement. Mullman et al. (1998a)

Table 6. Transition probabilities and oscillator strengths for Co II lines. $XE + Y$ stands for $X \times 10^{Y}$. Only transitions between experimentally known energy levels with log $gf \geq -4.0$ are listed in the table. The full table is available online.

λ^a (nm)	Lower level^b			Upper level^b			HFR+CPOL^c		
	E (cm^{-1})	Parity	J	E (cm^{-1})	Parity	J	log gf	gA (s^{-1})	CF
114.794	0	(e)	4	87 112	(o)	4	−3.04	4.64E+06	0.058
115.014	950	(e)	3	87 896	(o)	3	−3.20	3.20E+06	0.051
115.180	1597	(e)	2	88 418	(o)	2	−3.30	2.53E+06	0.056
116.231	1597	(e)	2	87 633	(o)	3	−3.78	8.16E+05	0.027
117.587	0	(e)	4	85 044	(o)	3	−3.50	1.51E+06	0.171
118.741	0	(e)	4	84 217	(o)	3	−1.01	4.61E+08	0.316
118.849	0	(e)	4	84 141	(o)	4	−1.63	1.10E+08	0.098
119.242	0	(e)	4	83 863	(o)	3	−2.94	5.32E+06	0.016
119.386	3350	(e)	5	87 112	(o)	4	−3.89	6.09E+05	0.039
119.841	950	(e)	3	84 395	(o)	2	−1.18	3.07E+08	0.359
...	...	...	...	...	...	...	...	...	...

[a]Vacuum ($\lambda < 200$ nm) and air ($\lambda > 200$ nm) Ritz wavelengths deduced from the experimental energy level values compiled at NIST (Kramida et al. 2014).
[b]From the NIST data base (Kramida et al. 2014). For commodity, energy values have been rounded to the nearest unit in the table; for more accurate values, see the NIST compilation.
[c]This work.

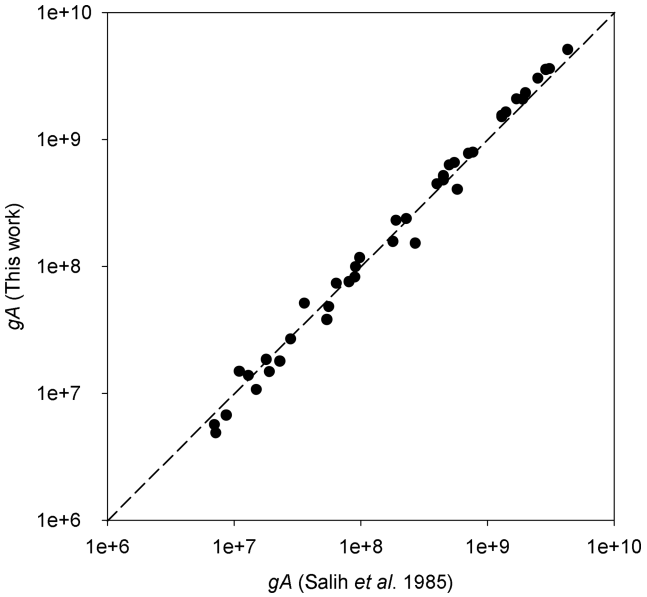

Figure 2. Comparison between the transition probabilities (gA in s^{-1}) calculated in the present work and those deduced from the experimental measurements due to Salih et al. (1985).

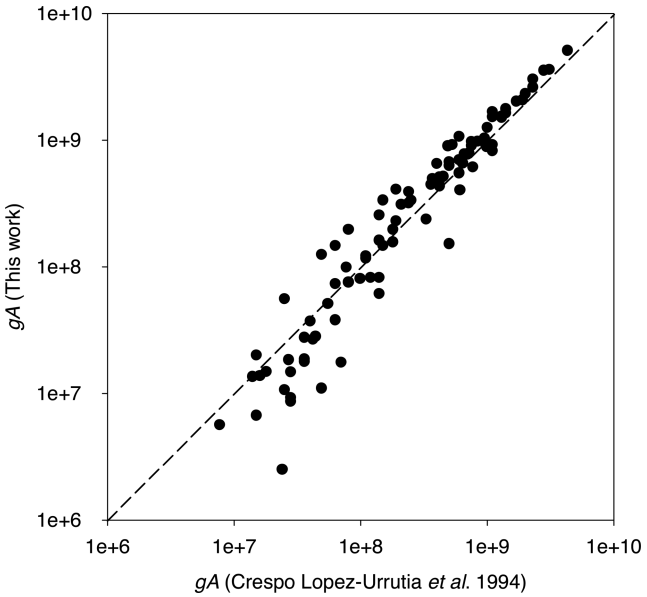

Figure 3. Comparison between the transition probabilities (gA in s^{-1}) calculated in the present work and those deduced from the experimental measurements due to Crespo López-Urrutia et al. (1994).

reported 28 oscillator strengths for ultraviolet Co II lines deduced from laser-induced fluorescence lifetimes and branching fraction measurements using a high-resolution grating spectrometer and an optically thin hollow cathode discharge. As illustrated in Fig. 4, our gf-values were found to agree in general within 20–30 per cent with the results obtained by Mullman et al. (1998a). More particularly, the mean ratio $gf_{\rm Thiswork}/gf_{\rm Mullman}$ was found to be equal to 1.339 ± 0.552 when using all the common lines, and to 1.238 ± 0.411 when using the strongest transitions for which log $gf > -1$. Finally, Fig. 5 shows the comparison between our computed oscillator strengths and those published by Raassen et al. (1998) who used the theoretical method of orthogonal operators to determine the log gf-values for ($3d^8$+$3d^7$4s)–$3d^7$4p transitions in Co II. In this case, the two sets of data generally agree within about 20 per cent, this percentage difference being reduced to 12 per cent when considering the most intense transitions with log $gf > -1$. We also note that our oscillator strengths are on average larger than those obtained by Raassen et al. This could be due to the fact that these latter authors included explicitly a less extended set of interacting configurations in their model.

5 CONCLUSION

Transition probabilities and oscillator strengths have been obtained for 5080 spectral lines in Co II using the pseudo-relativistic Hartree–Fock method including the most important intravalence correlation and core-polarization effects. The accuracy of the new data has been assessed through detailed comparisons with previously published experimental and theoretical radiative rates together with new lifetime measurements performed in the present work using the laser-induced fluorescence technique with one- and two-step excitations. In view of the overall agreement obtained between all

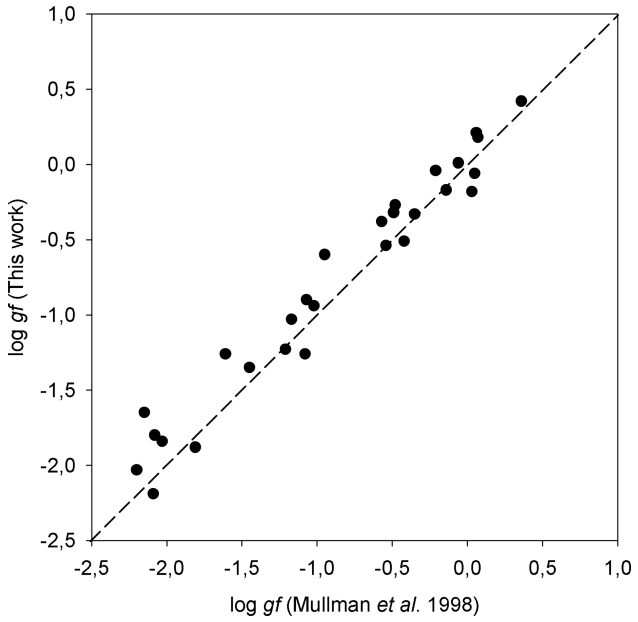

Figure 4. Comparison between the oscillator strengths (log *gf*) calculated in the present work and those deduced from the experimental measurements due to Mullman et al. (1998a).

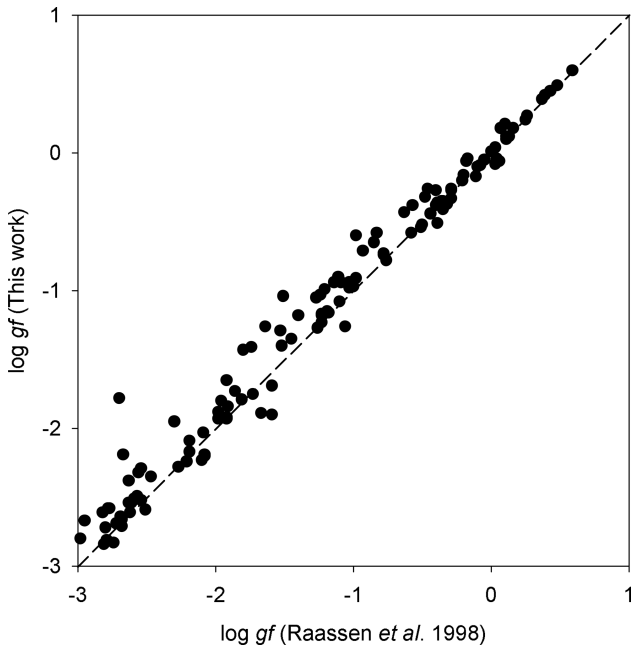

Figure 5. Comparison between the oscillator strengths (log *gf*) calculated in the present work and those computed by Raassen et al. (1998).

sets of results, it is expected that the new *gA*- and *gf*-values should be accurate to a few per cent for the strongest transitions and to within 20–30 per cent for weaker lines.

ACKNOWLEDGEMENTS

This work was financially supported by the Integrated Initiative of Infrastructure Project LASERLAB-EUROPE, contract LLC002130, by the Belgian F.R.S.-FNRS, and by the Swedish Research Council through the Linnaeus grant to the Lund Laser Centre and the Knut and Alice Wallenberg Foundation. PQ and PP are, respectively, Research Director and Research Associate of the F.R.S.-FNRS., VF is currently a post-doctoral researcher of the Return Grant program of the Belgian Scientific Policy (BELSPO) and HH gratefully acknowledges the grant no. 621-2011-4206 from the Swedish Research Council. The Belgian team is grateful to the Swedish colleagues for the warm hospitality enjoyed at the Lund Laser Centre during the two campaigns in 2015 June and August.

REFERENCES

Battistini C., Bensby T., 2015, A&A, 577, A9
Bravo E., Martinez-Pinedo G., 2012, Phys. Rev. C, 85, 055805
Cowan R. D., 1981, The Theory of Atomic Structure and Spectra. California Univ. Press, Berkeley
Crespo López-Urrutia J. R., Ulbel M., Neger T., Jäger H., 1994, J. Quant. Spectrosc. Radiat. Transf., 52, 89
Engström L., Lundberg H., Nilsson H., Hartman H., Bäckström E., 2014, A&A, 570, A34
Fraga S., Karwowski J., Saxena K. M. S., 1976, Handbook of Atomic Data. Elsevier, Amsterdam
Iglesias L., 1979, Opt. Pura Aplicada, 12, 63
Kramida A., Ralchenko Yu., Reader J., NIST ASD Team, 2014, NIST Atomic Spectra Database. Available at: http://physics.nist.gov/asd
Kurucz R., 2011, Available at: http://kurucz.harvard.edu/atoms/2801/gf2801.life
Lawler J. E., Sneden C., Cowan J. J., 2015, ApJS, 220, 13
Lind K., Bergemann M., Asplund M., 2012, MNRAS, 427, 50
Lundberg H. et al., 2016, MNRAS, 460, 356
Mullman K. L., Cooper J. C., Lawler J. E., 1998a, ApJ, 495, 503
Mullman K. L., Lawler J. E., Zsargó J., Federman S. R., 1998b, ApJ, 500, 1064
Nave G., Sansonetti C. J., 2011, J. Opt. Soc. Am. B, 28, 737
Pagel B. E. J., 2009, Nucleosynthesis and Chemical Evolution of Galaxies. Cambridge Univ. Press, Cambridge
Palmeri P., Quinet P., Fivet V., Biémont E., Nilsson H., Engström L., Lundberg H., 2008, Phys. Scr., 78, 015304
Pickering J. C., 1998, Phys. Scr., 58, 457
Pickering J. C., Raassen A. J. J., Uylings P. H. M., Johansson S., 1998, ApJS, 117, 261
Pinnington E. H., Lutz H. O., Carriveau G. W., 1973, Nucl. Instrum. Methods, 110, 55
Pinnington E. H., Lutz H. O., Carriveau G. W., 1974, Z. Phys., 267, 27
Quinet P., Palmeri P., Biémont E., McCurdy M. M., Rieger G., Pinnington E. H., Wickliffe M. E., Lawler J. E., 1999, MNRAS, 307, 934
Quinet P., Palmeri P., Biémont E., Li Z. S., Zhang Z. G., Svanberg S., 2002, J. Alloys Compounds, 344, 255
Raassen A. J. J., Pickering J. C., Uylings P. H. M., 1998, A&AS, 130, 541
Salih S., Lawler J. E., Whaling W., 1985, Phys. Rev. A, 31, 744
Sørensen G. J., 1979, Phys. (Paris) Colloques, 40, C1-190
Woosley S. E., Weaver T. A., 1995, ApJS, 101, 181

SUPPORTING INFORMATION

Additional Supporting Information may be found in the online version of this article:

Table 6. Transition probabilities and oscillator strengths for Co II lines.
(http://www.mnras.oxfordjournals.org/lookup/suppl/doi:10.1093/mnras/stw1900/-/DC1).

Please note: Oxford University Press is not responsible for the content or functionality of any supporting materials supplied by the authors. Any queries (other than missing material) should be directed to the corresponding author for the article.

This paper has been typeset from a TEX/LATEX file prepared by the author.